EXPERIMENTAL STUDY OF LOW-SPEED CAVITY FLOW USING STEADY JETS

Alhaddabi N.* ,Kontis K., Zare-Behtash H.
*Author for correspondence
School of Engineering
University of Glasgow
Glasgow, G12 8QQ,
United Kingdom,
E-mail: n.al-haddabi.1@research.gla.ac.uk

ABSTRACT

Open cavity ($L/D = 4$) was examined at low speed ($U_\infty = 26\ m/s$). The baseline flow showed a typical open cavity flow. It was also found that a region of relatively high velocity fluctuations (indicated by RMS values) extends along the cavity separated shear layer from the mid of the cavity to the cavity's trailing edge. Steady jets at an outlet velocity of 1.8 m/s was forced through a narrow slot at the leading edge. The jets modified the profile shape of the averaged U velocity for the shear layer at the close proximity of the leading edge. However, the jet increased the fluctuation in the separated shear layer.

NOMENCLATURE

B_c	[%]	Blowing coefficient
D	[m]	Cavity depth
H	[m]	Cavity depth
L	[m]	Cavity length
Re_h	[-]	Reynolds number based on slot's height
Re_x	[-]	Reynolds number based on spanwise distance
Re_θ	[-]	Reynolds number based on momentum thickness
RMS	[-]	Root-mean square value
U	[m/s]	Streamwise velocity
U_{jet}	[m/s]	Jet's average velocity
U_∞	[m/s]	Free stream velocity
V	[m/s]	Crosswise velocity
W	[m]	Cavity span
δ	[m]	Displacement thickness
θ	[m]	Momentum thickness
x	[m]	Streamwise distance
y	[m]	Crosswise distance
z	[m]	Spanwise distance

INTRODUCTION

In open cavities, the natural instability of the separated shear layer in addition to the feedback from the cavity trailing edge greatly organise/enhance the separated shear layer oscillations. This can lead to higher levels of induced drag, radiated noise and structural vibration. These issues challenge wide range of engineering applications, such as weapon bays, landing gears, slotted wall wind or water tunnel, slotted-flumes, bellow-type pipe configuration, high-head gates, gate slots and aircraft components and even ground and underwater applications [1].

As illustrated in Figure 1, the flow field in open cavity is dominated by the separated shear layer that separates at the cavity leading edge due to the geometrical discontinuity [2]. Due to the viscous and the strong turbulent transfer of momentum, the separated shear layer expands along the cavity [3]. As a result of this strong growth, portion of the separated shear layer impinge on the cavity trailing edge.

When the free stream velocity or the cavity length exceeds a certain threshold, the cavity separated shear layer become unstable [4]. In the vicinity of the separation region, the layer profile undergoes substantial change from the boundary layer profile to unstable hyperbolic profile [5] which is responsible for the K-H instability. The K-H instability generates instability waves that is amplified along the cavity and eventually they may roll into discrete large coherent vortices [6]. These coherent structures grow exponentially near the leading edge region, linearly along large portion of the cavity, then the growth diminish in the proximity of the cavity trailing edge [3]. Next to the trailing edge, the vortical structure may impinge, partially-impinge, or completely escape the trailing edge. This transverse variation in the vortex shedding street, observed by Kinsley and Rockwell [6], is interpreted as the flapping of the separated shear layer. The separated shear layer oscillations can be further enhanced naturally via one of three mechanisms, which are: hydrodynamic feedback, acoustic feedback, and displacement of the cavity solid boundaries [1].
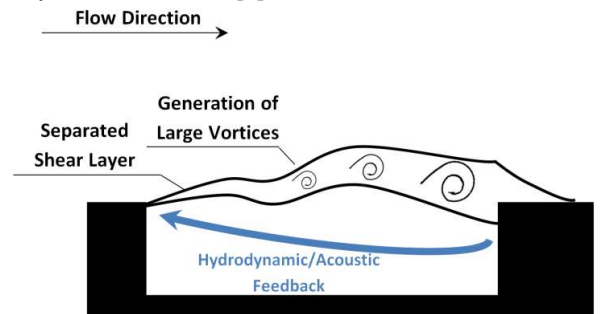

Figure 1 Mechanism of the separated shear layer oscillations in open cavities

The objective of this study is to study the effect of a steady parallel jet (see figure 2) on the mean flow field of the cavity.
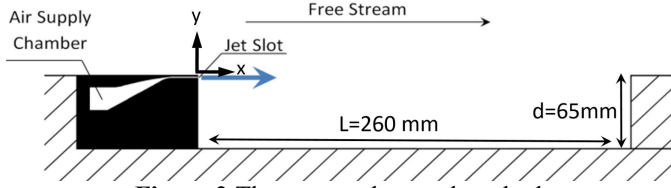

Figure 2 The proposed control method

EXPERIMENTAL MODEL

The experiments were carried out in De Havilland tunnel, which is owned by University of Glasgow. The tunnel is closed-return wind tunnel, which has maximum wind speed of 76 m/s. The test section is hexagonal, and it is 2.1 m high, 2.7 m wide and 5.6 m long. The wind tunnel is derived by 3 m-diameter fan. 5 cm wide vent gap is located downstream of the test section to maintain the wind tunnel at the atmospheric pressure. The tunnel is also equipped with honeycombs and fine meshes upstream of the test section in order to reduce turbulence intensity to the desired level. The turbulence intensity at the center of the test section of the current tunnel is nearly 0.4% for free stream velocities from 10-25 m/s. Pitot tube and a thermocouple were used to monitor the air velocity and temperature upstream of the model.

The model was made of wooden panels and painted black in order to minimise laser reflections for laser-based methods. The model top surface is 0.98 m above the floor of the test section. The length of the cavity (L) can be varied to achieve L/D=4,12 and 20 by removing number of filler boxes. In this paper, we only consider open cavity case. The spanwise width (W) of the cavity is 0.8m, while the L/W ratio for the current cavity is 0.325. Two inter-changeable endplates (2.89 m-long, 0.560 mm-high) were attached to the model sides. One of them is made of clear Perspex to allow light access and the second is made of wood to minimize cost and provide support to the Perspex endplate via two symmetrical slim airfoils, which are not interfering with the flow under study. The airfoils were made of carbon fiber sheets and epoxy. The model was carried above the test section floor using four carbon fiber legs. Each leg is attached with 12.5 mm-thick aluminum plate in each side in order to attach the leg to the model and the test section floor. The blockage ratio (based on the ratio of the cross sectional area of the model to that of the test section) is approximately 5.9%.

As illustrated in Figure 2, the point of the coordinate system for all measurements is at the leading edge. The x-axis is parallel to the free stream while the y-axis is perpendicular to the x- axis. The z-axis is parallel to the jet slot.

TEST CONDITIONS

The tests were carried out at a free stream of 26 m/s. The jet's slot in the current experiments is approximately 0.4 m-wide and 1.85 mm-high. The blowing coefficient, is defined by

$$B_c = \frac{\rho_{jet}\, U_{jet}\, A_{jet}}{\rho_\infty\, U_\infty\, A_{cavity}}$$

where $\rho_{jet}, U_{jet}, A_{jet}$ are jet density, jet velocity and slot area per unit width. On the other hand, $\rho_\infty, U_\infty, A_{cavity}$ are free stream density, free stream velocity and cavity floor area per unit width. Table 1 shows parameter related to the jet used to control the flow. A hand-held digital wind speed anemometer was used to measure the jet's average velocity and to confirm the two-dimensionality of the jet in the spanwise direction.

Table 1 parameters of the steady-jet case

U_{jet}	B_c	Re_h
1.8 m/s	0.21%	2.54×10^2

PIV was utilized to plot the boundary layer upstream of the cavity at $x/L = -0.05$. Table 2 shows the parameter of the upstream boundary layer. 13 vectors were used to resolve the boundary layer profile. The thickness of the boundary layer (based on the $U = 0.99\, U_\infty$) is around 16.5 mm.

Table 2 Boundary layer parameters

δ	Re_δ	θ	Re_θ
16.5 mm	30×10^3	2.1 mm	3.8×10^3

EXPERIMENTAL SET-UP

Lavision Planar PIV system was used to study the velocity field. Laser was emitted using Litron double cavity Nd:YAG, Q-switched laser, which has a maximum pulse energy output of 2000 mJ at a repetition rate of around 2.5 Hz. The 532 nm laser is guided to the top optical access of the test section via number of fixed mirrors and a guiding arm. The laser sheet was illuminated at the centerline of the cavity covering the entire cavity length and portion of the areas upstream and downstream of the cavity.

Pro X 11 Megapixel camera with a CCD chip of 4008 x 2672 pixels and 9 μm pixel size was positioned orthogonal to the laser sheet. The focus of the camera was adjusted using 200 mm Canon lens. A 300 mmx300 mm Lavision model calibration plate was used to calibrate the raw images. The root-mean-square of the mapping function fit (the average deviation of the distorted mark positions from the ideal grid) for all the calibrations were less than 0.7, which is good value for calibration.
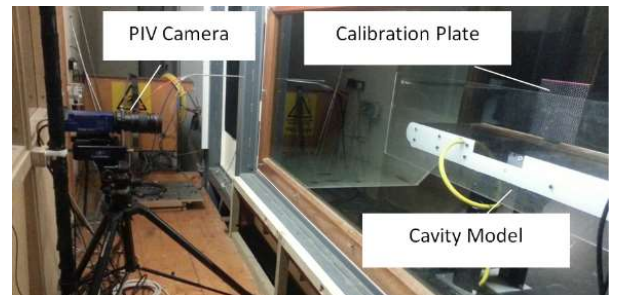

**Figure 3** The PIV camera was orthogonal to the laser sheet

For each case, a total of 800 images were recorded by the camera. DaVis 7.2 software was used to process all the raw images. Cross correlation mode was used to correlate each image pair. Each image consists of two frames (frame 0 for the 1st exposure and frame 1 for the 2nd exposure). Each frame is divided into number of integration windows. The cross correlation was computed for all the integration areas for frame 0 and 1. The highest peak in the cross-correlation image is expected to be the displacement vector.

Multi-pass (two passes with decreasing window size from 64x64 pixel^2 to 32x32 pixel^2) correlation was used to improve the special resolution and produce less erroneous vectors (DaVis, 2007). The overlap between the interrogation windows was 50% in order to improve the spatial resolution by reducing the grid size. This gave a final spatial resolution of 1 vector per 1.6x1.6 mm^2.

In addition, correlation peak validation was implemented to get rid of the erroneous vectors. The peak ratio (which is related to the ratio of the highest correlation peak to the second highest correlation peak) was set to be less than 1.3. The regional median filter is also applied, which compares the center vector with its neighboring vectors. In order to reduce noise, a simple 3x3 smoothing filter was applied on the final vector field.
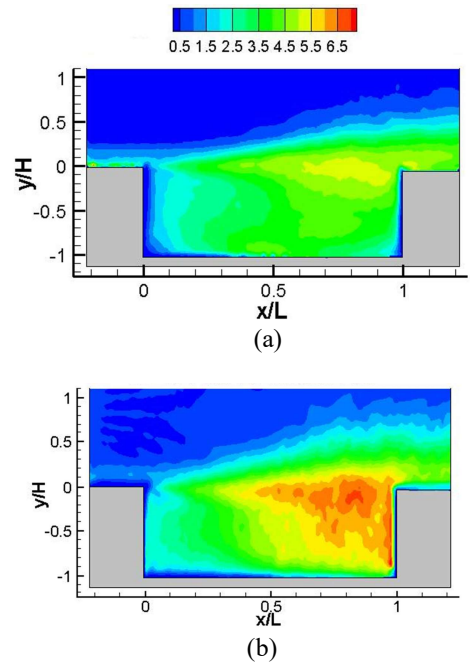
BASELINE CAVITY FLOW

Figure 4 shows the averaged-velocity streamlines for the baseline flow. The streamline shows the main features of the open cavity explained in the literature. It shows that the separated shear layer bridges the cavity and reattaches at the trailing edge. Two recirculation vortices appear in the recirculation region: a large clockwise vortex centered next to the trailing edge and dominates the recirculation region, a smaller anti-clockwise weak vortex centered in the proximity of the leading edge step.
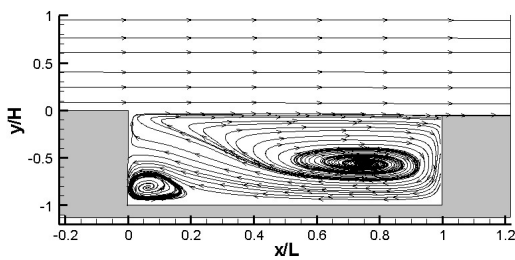
**Figure 4** Baseline cavity flow: averaged-velocity streamlines

Figure 5 shows the contour plots for time-averaged root mean square RMS for U_{rms} and V_{rms}. A region of relatively high velocity fluctuations (indicated by RMS values) extends from the mid of the cavity the along the cavity separated shear layer to the trailing edge. The size and the magnitude of the region increases as it approaches the cavity trailing edge. This increase is probably because of two elements, which were mentioned by Rossiter [7]. The first element is the random fluctuation generated due to the interaction of the separated layer with the trailing edge. The second element is the growth of the coherent vortical structures in the streamwise direction.

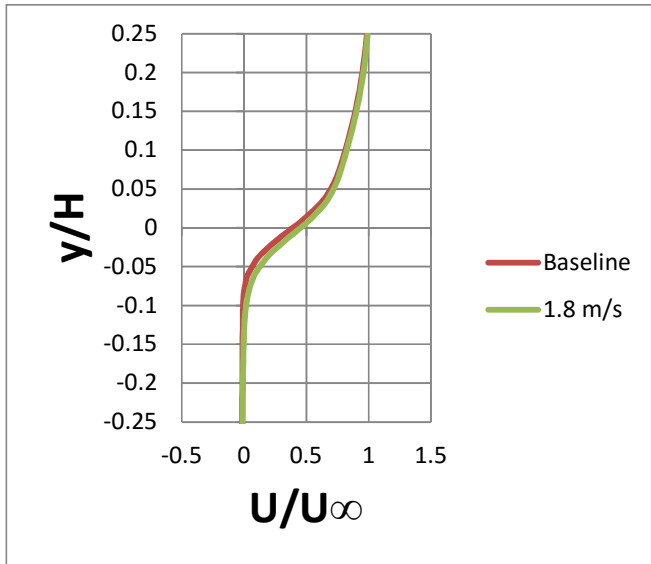**Figure 5** Contour plots for time-averaged RMS for: a) U_{rms}, b) V_{rms}

CONTROLLED CAVITY FLOW

Figure 6 shows the Averaged U velocity for the baseline flow and the steady-jet case. No significant effect by the jet was observed on the cavity flow topology.
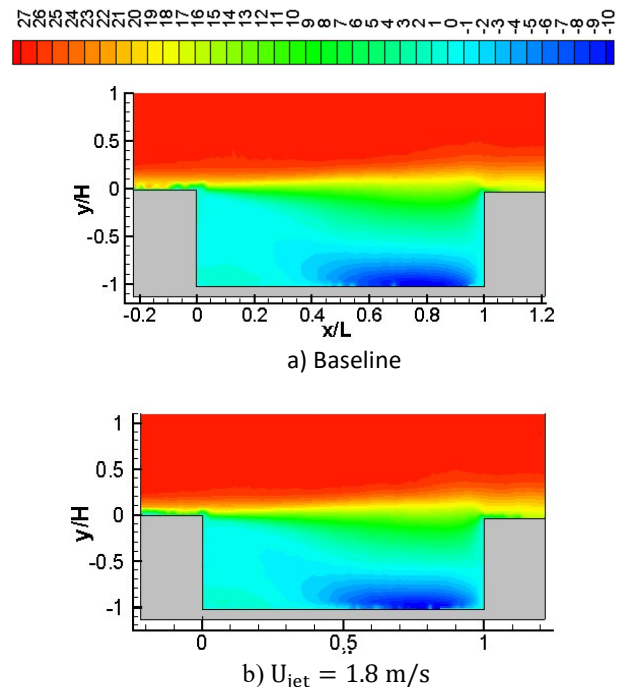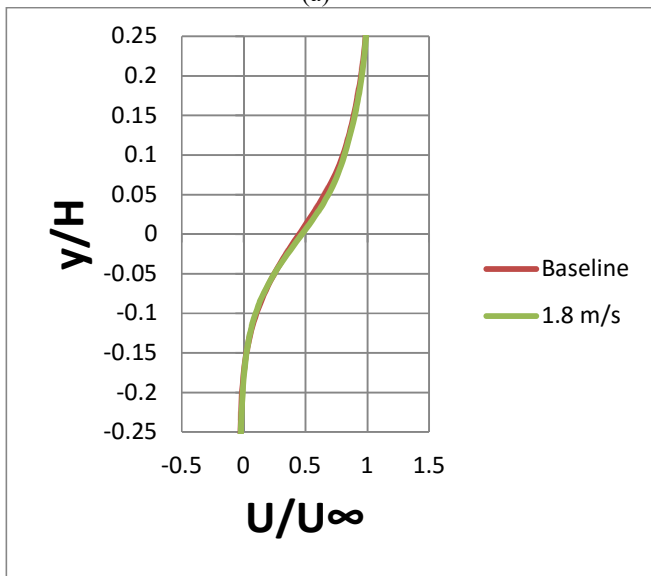
Figure 6 Averaged U velocity for the baseline flow and the steady-jet case

Averaged U velocity profiles at the separated shear layer for streamwise stations $x/L = 0.05$ and $x/L = 0.2$ for the baseline and the steady-jet case are shown in Figure 7. At $x/L = 0.05$, the jet causes the velocity profile to shift slightly. As the jet expands and mixes with cavity flow, this effect diminishes at $x/L = 0.1$.


(a)

(b)

Figure 7 Averaged U velocity profiles at a) $x/L = 0.05$, b) $x/L = 0.2$ for the baseline and the steady-jet case.

On the other hand, the contour plots for time-averaged RMS magnitude for the streamwise velocity fluctuations are shown in Figure 8. The figure indicates that the separated shear layer fluctuations for the steady-jet case is higher than those for the baseline flow. This increase is perhaps due to the additional turbulence generated by the interaction between the jet and the separated shear layer.
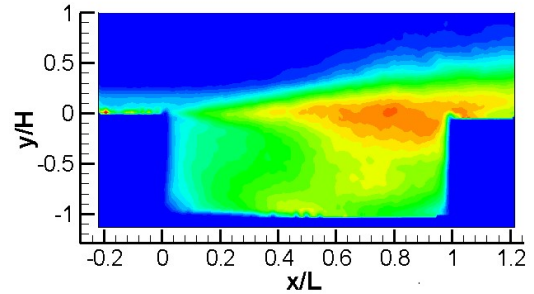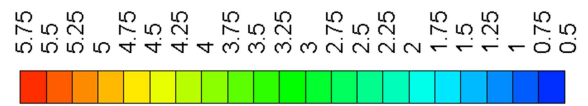
a) baseline
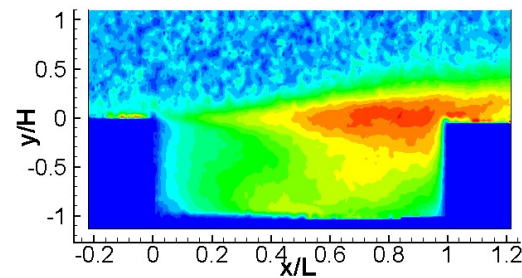
b) $U_{jet} = 1.8$ m/s

Figure 8 Contour plots for time-averaged U_{rms} for baseline flow and the steady-jet case

CONCLUSIONS

Open cavity $(L/D = 4)$ was examined at low speed $(U_\infty = 26\ m/s)$. The upstream boundary layer was around 16.5 mm thick, while the Reynolds number based on length was $Re_x = 1.1 \times 10^6$. Low-repetition rate PIV system was used to compute the velocity field for the flow. The baseline flow showed a typical open cavity flow. The separated shear layer expands transversely until it reattaches at the trailing edge, while two counter-rotating recirculation vortices appear in the recirculation region. It was also found that a region of relatively high velocity fluctuations (indicated by RMS values) extends along the cavity separated shear layer from the mid of the cavity to the cavity's trailing edge. The size and the magnitude of the region increases as it approaches the cavity trailing edge. This increase is perhaps due to the interaction between the separated shear layer and the trailing edge or due to the growth of the separated shear layer oscillations.

Steady jet was introduced through a narrow slot in the leading edge. The jets slightly modified the profile shape of the averaged U velocity for the shear layer at the close proximity of the leading edge. However, this effect diminishes quickly downstream. In addition to this, the steady-jet case showed an increase in the streamwise fluctuation in the separated shear layer. This increase is perhaps due to the additional turbulence generated by the interaction between the jet and the separated shear layer.

REFERENCES

[1] Rockwell, D., & Naudascher, E. (1979). Self-sustained oscillations of impinging free shear layers. Annual Review of Fluid Mechanics, 11(1), 67-94.

[2] Ng, Y. T. (2012). Characterising low-speed, transitional cavity flow. Aeronautical Journal, 116(1185), 1185-1199.

[3] Ashcroft, G., & Zhang, X. (2005). Vortical structures over rectangular cavities at low speed. Physics of Fluids (1994-present), 17(1), 015104.

[4] Gharib, M. (1987). Response of the cavity shear layer oscillations to external forcing. AIAA journal, 25(1), 43-47.

[5] Gharib, M., & Roshko, A. (1987). The effect of flow oscillations on cavity drag. Journal of Fluid Mechanics, 177, 501-530.

[6] Knisely, C., & Rockwell, D. (1982). Self-sustained low-frequency components in an impinging shear layer. Journal of Fluid Mechanics, 116, 157-186.

[7] Rossiter, J. E. (1964). Wind tunnel experiments on the flow over rectangular cavities at subsonic and transonic speeds. Ministry of Aviation; Royal Aircraft Establishment; RAE Farnborough.